

Dinuclear Valence Tautomeric 1,2-Semiquinonato/Catecholato-cobalt Complexes Containing 1,1,4,7,10,10-Hexamethyltriethylenetetramine

Hui Liang,¹ Young Mee Na,¹ In Sung Chun,¹ Soon Sik Kwon,¹ Young-A Lee,² and Ok-Sang Jung*¹

¹Department of Chemistry, Pusan National University, Pusan 609-735, Korea

²Department of Chemistry, Chonbuk National University, Jeonju 561-756, Korea

Received September 27, 2006; E-mail: oksjung@pusan.ac.kr

Dinuclear 1,2-semiquinonato/catecholato-cobalt complexes containing 1,1,4,7,10,10-hexamethyltriethylenetetramine (hmdeta) as a potential tetradentate N₄ coligand, [Co₂(hmteta)(dbbq)₄], (dbbq = 3,5- and 3,6-di-*tert*-butyl-1,2-benzoquinone (3,5-dbbq and 3,6-dbbq)) were synthesized and characterized. The crystal structures proved that [Co₂(hmteta)(3,6-dbbq)₄]·2C₆H₅CH₃ ([3,6]) exists as low spin [(3,6-dbsq)(3,6-dbcate)Co^{III}(hmteta)Co^{III}(3,6-dbsq)(3,6-dbcate)] (3,6-dbsq = 3,6-di-*tert*-butyl-1,2-semiquinonato; 3,6-dbcate = 3,6-di-*tert*-butylcatecholato), while [Co₂(hmteta)(3,5-dbbq)₄]·C₆H₅CH₃ ([3,5]) approximates to [(3,5-dbsq)₂Co^{II}(hmteta)Co^{II}(3,5-dbsq)₂] in the solid state at ambient temperature. On the basis of the effective magnetic moments, the [Co^{III}] → [Co^{II}] conversion of [3,6] underwent a relatively abrupt transition around 330 K while that of [3,5] occurs in a wide range of temperature. Electronic absorption spectra showed that [3,6] shifts predominantly to [Co^{III}] whereas [3,5] shifts to [Co^{II}] valence tautomer in solution at room temperature. The charge distribution of [3,6] exhibited significant solvent effects at room temperature. These prominent features between [3,5] and [3,6] appeared to be associated with difference between delicate electronic and steric effects of the two dbbq ligands.

Electronic-labile complexes can be used as potential building blocks for molecular electronic devices.^{1–3} An external perturbation on these complexes should lead to an interconversion between two nearly degenerate states. Transition-metal coordination complexes that contain bistable components^{4–7} have been the subject of intensive research for memory and storage materials, sensors, and molecular switches.^{8,9} In particular, metal complexes containing 1,2-semiquinonato (sq^{•−}, *S* = 1/2) and catecholato (cat^{2−}, *S* = 0) ligands have shown a unique bistability via the intramolecular electron transfer between the metal and ligand around room temperature.¹⁰ This has been most remarkably illustrated for the cobalt complexes where temperature- and photo-dependent equilibria between [Co^{III}] and [Co^{II}] valence tautomers have been observed both in solution and in the solid state (Eq. 1).^{11,12} Equilibria between [Co^{III}] and [Co^{II}] tautomers via the shift from low spin



Co^{III} to high spin Co^{II} have been monitored by the effective magnetic moments and electronic spectral changes. A decrease in the temperature leads to a stabilization of the [Co^{III}] tautomer. In relation to the bistable valence tautomerism, unique physicochemical properties, such as the presence of the characteristic band near 2500 nm (4000 cm^{−1}) for [Co^{III}] tautomer, crystal bending effect, and huge hysteresis, have been observed.^{13–17} These phenomena are a consequence of charge localization within the molecule and the close energy separation between localized quinone and cobalt electronic levels.¹⁸ Our previous results show that valence tautomerism is very sensitive to light, solvent, or state as well as partial change of the diimine (N–N) coligands.^{13–17}

However, dinuclear analogues remain unexplored except for two examples.^{16,19} Dinuclear valence tautomers may possess various stable or metastable states, such as [Co^{III}]₂, [Co^{II}][Co^{III}], [Co^{II}]₂, which may be useful for ternary information storage at molecular level.¹⁹ In order to obtain the dinuclear valence tautomeric analogues, 1,1,4,7,10,10-hexamethyltriethylenetetramine (hmteta) (Chart 1) was used as a ligand. The first goal was to synthesize the dinuclear valence tautomeric complexes, and the second goal was to directly compare the properties induced by the difference between 3,5-di-*tert*-butyl-1,2-benzoquinone (3,5-dbbq) and 3,6-di-*tert*-butyl-1,2-benzoquinone (3,6-dbbq). Herein, we report the synthesis, structures, and physicochemical properties of new dinuclear valence tautomeric cobalt complexes.

Experimental

Materials and Measurements. Octacarbonyldicobalt [Co₂(CO)₈] was purchased from Strem. 3,5-Di-*tert*-butyl-1,2-benzoquinone (3,5-dbbq) and 1,1,4,7,10,10-hexamethyltriethylenetetramine (hmteta) were purchased from Aldrich. 3,6-Di-*tert*-butyl-1,2-benzoquinone (3,6-dbbq) was prepared according to the literature procedure.²⁰ Elemental analysis (C,H,N) was carried out at the Advanced Analysis Center, KBSI. Infrared spectra were obtained in 5000–400 cm^{−1} range on a Perkin-Elmer 16F PC FT-IR spectrophotometer with samples prepared as KBr pellets.

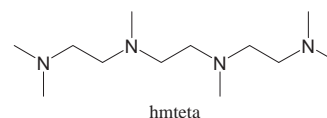


Chart 1.

Table 1. Crystallographic Data for [3,5] and [3,6]

| | Co ₂ (hmteta)(3,5-dbbq) ₄ ·C ₆ H ₅ CH ₃ | [Co ₂ (hmteta)(3,6-dbbq) ₄]·2C ₆ H ₅ CH ₃ |
|---|--|---|
| Formula weight | 1321.59 | 1413.73 |
| Space group | $P\bar{1}$ (No. 2) | $P\bar{1}$ (No. 2) |
| <i>a</i> , <i>b</i> , <i>c</i> /Å | 10.662(3), 11.140(3), 16.964(5) | 11.937(2), 12.240(3), 14.369(3) |
| α , β , γ /° | 92.576(6), 93.295(6), 113.654(5) | 109.998(4), 98.508(4), 93.051(4) |
| <i>V</i> /Å ³ | 1837.5(9) | 1938.9(7) |
| <i>Z</i> | 1 | 1 |
| <i>D</i> _{calcd} /Mg m ⁻³ | 1.194 | 1.211 |
| Abs. coeff./mm ⁻¹ | 0.506 | 0.484 |
| <i>F</i> (000) | 714 | 764 |
| Crystal size/mm ³ | 0.40 × 0.20 × 0.02 | 0.25 × 0.20 × 0.03 |
| θ_{\max} /° | 25 | 26 |
| Index ranges | ± <i>h</i> , ± <i>k</i> , ± <i>l</i> | ± <i>h</i> , ± <i>k</i> , ± <i>l</i> |
| Refls collected | 10473 | 11455 |
| Indep. reflections | 7305 [<i>R</i> (int) = 0.0946] | 7766 [<i>R</i> (int) = 0.0718] |
| Parameters refined | 415 | 421 |
| Goodness of fit | 0.984 | 0.888 |
| <i>R</i> indices [<i>I</i> > 2σ(<i>I</i>)] ^{a)} | <i>R</i> 1 = 0.0753, <i>wR</i> 2 = 0.1570 | <i>R</i> 1 = 0.0602, <i>wR</i> 2 = 0.1243 |
| <i>R</i> indices (all data) | <i>R</i> 1 = 0.1935, <i>wR</i> 2 = 0.2136 | <i>R</i> 1 = 0.1456, <i>wR</i> 2 = 0.1484 |
| Largest diff. peak and hole/eÅ ⁻³ | 0.591 and -1.035 | 0.559 and -0.528 |

a) $R1 = ||F_o| - |F_c||/|F_o|$, $wR2 = \{(F_o^2 - F_c^2)^2/wF^4\}^{1/2}$.

Temperature-dependent magnetic measurements were made on a Quantum Design MPMS-5 SQUID magnetometer. Electronic spectra were recorded on a Perkin-Elmer Lambda 9 spectrophotometer. Differential scanning calorimetry (DSC) and thermogravimetric analysis (TGA) were performed by using a Stanton Red Croft TG 100 with a scanning rate of 10 °C min⁻¹.

[Co₂(hmteta)(3,5-dbbq)₄] ([3,5]). Co₂(CO)₈ (86 mg, 0.25 mmol) and 3,5-dbbq (220 mg, 1.0 mmol) were combined in 15 mL of toluene. The mixture was stirred for 5 min, and hmteta (57.5 mg, 0.25 mmol) dissolved in 15 mL of toluene was added into the solution. The solution was stirred for 2 h at room temperature. Evaporation of the solvent gave a dark blue product in 93% yield. Single crystals suitable for crystallographic characterization were obtained in toluene solution at 5 °C. Found: C, 68.30; H, 9.08; N, 4.27%. Calcd for C₆₈H₁₁₀N₄O₈Co₂·C₆H₅CH₃: C, 68.16; H, 9.00; N, 4.24%. IR (KBr, cm⁻¹): 4152(br, s), 2956(s), 1579(m), 1460(s), 1355(m), 984(s), 899(m), 688(s), 494(m).

[Co₂(hmteta)(3,6-dbbq)₄] ([3,6]). The product was obtained by the same procedure, using 3,6-dbbq instead of 3,5-dbbq. The complex was obtained in 94% yield. Dark blue crystals suitable for crystallographic characterization were obtained in toluene at 5 °C. Found: C, 69.40; H, 9.01; N, 4.02%. Calcd for C₆₈H₁₁₀N₄O₈Co₂·2C₆H₅CH₃: C, 69.65; H, 8.99; N, 3.97%. IR (KBr, cm⁻¹): 3835(br, s), 2951(s), 1474(m), 1277(m), 953(s).

X-ray Crystallography. X-ray data were collected on a Bruker SMART automatic diffractometer with a graphite-monochromated Mo Kα radiation ($\lambda = 0.71073$ Å) and a CCD detector at ambient temperature. A list of 45 frames of two-dimensional diffraction images were collected and processed to obtain the cell parameters and orientation matrix. The data were corrected for Lorentz and polarization effects. Absorption effects were corrected by the empirical ψ -scan method. The structures were solved by the direct method (SHELXS 97) and refined by full-matrix least-squares techniques (SHELXL 97).²¹ The non-hydrogen atoms were refined anisotropically, and hydrogen atoms were placed in calculated positions and refined only for the isotropic thermal factors. Solvate toluene molecules were disordered. Crystal parameters and procedural information corresponding to data collection

and structure refinement are given in Table 1.

Crystallographic data have been deposited with Cambridge Crystallographic Data Centre: Deposition numbers CCDC-620884 and -620885. Copies of the data can be obtained free of charge via <http://www.ccdc.cam.ac.uk/conts/retrieving.html> (or from the Cambridge Crystallographic Data Centre, 12, Union Road, Cambridge, CB2 1EZ, UK; Fax: +44 1223 336033; e-mail: deposit@ccdc.cam.ac.uk).

Results and Discussion

Synthesis. The dinuclear cobalt complexes were synthesized in quantitative yields using a potential tetradentate instead of simple bidentate coligands according to the procedures described in earlier studies:^{13,22,23} the reaction between [Co₂(CO)₈] and 3,6-dbbq in the presence of 1,1,4,7,10,10-hexamethyltriethylenetetramine (hmteta) in toluene at room temperature afforded the present complexes. The solid products were recrystallized in toluene to give crystals suitable for single crystal X-ray crystallography and satisfactory chemical analyses. The products were soluble in common solvents such as toluene, benzene, tetrahydrofuran, acetone, dimethylsulfoxide, and dimethylformamide. This facile synthesis was attributed to the solubility of the dinuclear complexes in toluene. However, the compounds easily dissociated in dimethylsulfoxide or dimethylformamide. This solubility supports that the complexes are discrete molecules. The dinuclear cobalt complexes were characterized based on spectral, thermal, and magnetic properties along with crystal structures.

Crystal Structures. Dark blue crystals of the two complexes were obtained as toluene solvates. ORTEP views of [Co₂(hmteta)(3,5-dbbq)₄]·C₆H₅CH₃ and [Co₂(hmteta)(3,6-dbbq)₄]·2C₆H₅CH₃ are shown in Figs. 1 and 2, respectively, and relevant bond lengths and angles are listed in Table 2. For [3,6], the bond lengths of Co–O (1.852(3)–1.890(3) Å) were shorter than general Co^{II}–O bonds (≥ 2.00 Å). The Co–N distances (2.025(4) and 2.054(4) Å) were also shorter than

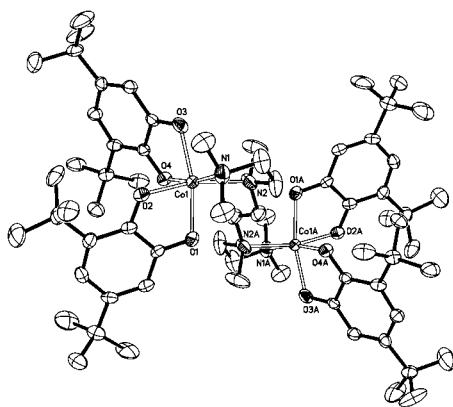


Fig. 1. ORTEP view of $[\text{Co}_2(\text{hmteta})(3,5\text{-dbbq})_4] \cdot \text{C}_6\text{H}_5\text{CH}_3$. H atoms and solvate molecules are omitted for clarity.

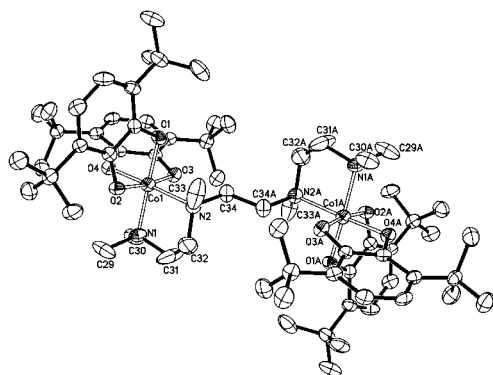


Fig. 2. ORTEP view of $[\text{Co}_2(\text{hmteta})(3,6\text{-dbbq})_4] \cdot 2\text{C}_6\text{H}_5\text{CH}_3$. H atoms and solvate molecules are omitted for clarity.

those of $[\text{Co}^{\text{II}}]$ species.¹⁵ The radius of a low spin Co^{III} ion has been reported to be roughly 0.2 Å shorter than the radius of a high spin Co^{II} ion.¹⁵ Thus, $[\text{Co}_2(\text{hmteta})(3,6\text{-dbbq})_4] \cdot 2\text{C}_6\text{H}_5\text{CH}_3$ is clearly a low spin $[\text{Co}^{\text{III}}]$ species with one 3,6-dbbq²⁻ and one 3,6-dbsq⁻ ligands. Moreover, oxygen atoms O(1) and O(2) ($\text{O}(1)\text{--C}(1) = 1.314(4)$ Å; $\text{O}(2)\text{--C}(6) = 1.323(5)$ Å) were associated with the 3,6-di-*tert*-butyl-1,2-semiquinonate (3,6-dbsq⁻, $S = 1/2$), and O(3) and O(4) ($\text{O}(3)\text{--C}(15) = 1.337(4)$ Å; $\text{O}(4)\text{--C}(20) = 1.332(4)$ Å) belong to 3,6-di-*tert*-butylcatecholate (3,6-dbbq²⁻, $S = 0$). Thus, the molecule is $[(3,6\text{-dbsq})(3,6\text{-dbbq})\text{Co}^{\text{III}}(\text{hmteta})\text{Co}^{\text{III}}(3,6\text{-dbsq})(3,6\text{-dbbq})]$ in the solid state at room temperature. The bond lengths and angles were similar to those of $[\text{Co}^{\text{III}}(3,6\text{-dbsq})(3,6\text{-dbbq})(\text{tmeda})]$ ($\text{Co}\text{--O} = 1.872(2)$; $\text{Co}\text{--N} = 2.026(2)$ Å).¹³ In contrast, for [3,5], the $\text{Co}\text{--O}$ bond lengths ($2.021(4)\text{--}2.043(4)$ Å) and $\text{Co}\text{--N}$ ($2.175(5)$, $2.179(5)$ Å) were much longer than those of [3,6]. The $\text{C}\text{--O}$ bond lengths ($\text{C}\text{--O} = 1.279(6)\text{--}1.297(6)$ Å) are much shorter than those of [3,6]. These facts indicated that [3,5] is basically to a $[(3,5\text{-dbsq})_2\text{Co}^{\text{II}}(\text{hmteta})\text{Co}^{\text{II}}(3,5\text{-dbsq})_2]$ in the solid state at room temperature. The geometry around the cobalt ion was severely distorted from a typical octahedral arrangement. A low spin Co^{III} ion is expected to be in a rigidly octahedral arrangement²⁴ in contrast to a few examples of the high spin Co^{II} trigonal prism.^{13,25} Thus, for [3,5], the distorted octahedral geometry around the cobalt ion may be additional evi-

Table 2. Selected Bond Lengths (Å) and Angles (deg) for [3,5] and [3,6]

| [3,5] | | [3,6] | |
|--|----------|--|-----------|
| $\text{Co}(1)\text{--O}(1)$ | 2.021(4) | $\text{Co}(1)\text{--O}(4)$ | 1.852(3) |
| $\text{Co}(1)\text{--O}(4)$ | 2.038(4) | $\text{Co}(1)\text{--O}(1)$ | 1.865(3) |
| $\text{Co}(1)\text{--O}(3)$ | 2.038(4) | $\text{Co}(1)\text{--O}(3)$ | 1.881(2) |
| $\text{Co}(1)\text{--O}(2)$ | 2.043(4) | $\text{Co}(1)\text{--O}(2)$ | 1.890(3) |
| $\text{Co}(1)\text{--N}(1)$ | 2.157(5) | $\text{Co}(1)\text{--N}(1)$ | 2.025(4) |
| $\text{Co}(1)\text{--N}(2)$ | 2.179(5) | $\text{Co}(1)\text{--N}(2)$ | 2.054(3) |
| $\text{O}(1)\text{--C}(1)$ | 1.282(6) | $\text{O}(1)\text{--C}(1)$ | 1.314(4) |
| $\text{O}(2)\text{--C}(2)$ | 1.297(6) | $\text{O}(2)\text{--C}(6)$ | 1.323(5) |
| $\text{O}(3)\text{--C}(15)$ | 1.279(6) | $\text{O}(3)\text{--C}(15)$ | 1.337(4) |
| $\text{O}(4)\text{--C}(16)$ | 1.290(6) | $\text{O}(4)\text{--C}(20)$ | 1.332(4) |
| $\text{O}(1)\text{--Co}(1)\text{--O}(4)$ | 88.9(2) | $\text{O}(4)\text{--Co}(1)\text{--O}(1)$ | 90.2(1) |
| $\text{O}(1)\text{--Co}(1)\text{--O}(3)$ | 166.1(2) | $\text{O}(1)\text{--Co}(1)\text{--O}(3)$ | 88.2(1) |
| $\text{O}(4)\text{--Co}(1)\text{--O}(3)$ | 79.5(2) | $\text{O}(4)\text{--Co}(1)\text{--O}(3)$ | 79.53(15) |
| $\text{O}(1)\text{--Co}(1)\text{--O}(2)$ | 79.8(2) | $\text{O}(4)\text{--Co}(1)\text{--O}(2)$ | 88.0(1) |
| $\text{O}(4)\text{--Co}(1)\text{--O}(2)$ | 89.1(2) | $\text{O}(1)\text{--Co}(1)\text{--O}(2)$ | 86.1(1) |
| $\text{O}(3)\text{--Co}(1)\text{--O}(2)$ | 92.2(2) | $\text{O}(3)\text{--Co}(1)\text{--O}(2)$ | 172.2(1) |
| $\text{O}(1)\text{--Co}(1)\text{--N}(1)$ | 101.6(2) | $\text{O}(4)\text{--Co}(1)\text{--N}(1)$ | 91.7(1) |
| $\text{O}(4)\text{--Co}(1)\text{--N}(1)$ | 169.3(2) | $\text{O}(1)\text{--Co}(1)\text{--N}(1)$ | 178.0(1) |
| $\text{O}(3)\text{--Co}(1)\text{--N}(1)$ | 89.8(2) | $\text{O}(3)\text{--Co}(1)\text{--N}(1)$ | 92.6(1) |
| $\text{O}(2)\text{--Co}(1)\text{--N}(1)$ | 90.9(2) | $\text{O}(2)\text{--Co}(1)\text{--N}(1)$ | 93.3(1) |
| $\text{O}(1)\text{--Co}(1)\text{--N}(2)$ | 80.0(2) | $\text{O}(4)\text{--Co}(1)\text{--N}(2)$ | 178.1(1) |
| $\text{O}(4)\text{--Co}(1)\text{--N}(2)$ | 98.5(2) | $\text{O}(1)\text{--Co}(1)\text{--N}(2)$ | 91.6(1) |
| $\text{O}(3)\text{--Co}(1)\text{--N}(2)$ | 100.3(2) | $\text{O}(3)\text{--Co}(1)\text{--N}(2)$ | 92.8(1) |
| $\text{O}(2)\text{--Co}(1)\text{--N}(2)$ | 166.4(2) | $\text{O}(2)\text{--Co}(1)\text{--N}(2)$ | 92.6(1) |
| $\text{N}(1)\text{--Co}(1)\text{--N}(2)$ | 83.8(2) | $\text{N}(1)\text{--Co}(1)\text{--N}(2)$ | 86.5(1) |

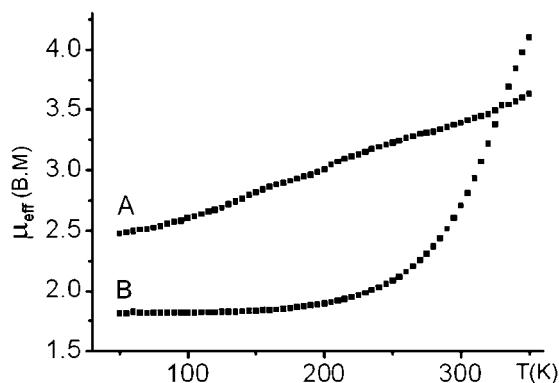


Fig. 3. Plots of magnetic moments of $[\text{Co}_2(\text{hmteta})(3,5\text{-dbbq})_4] \cdot \text{C}_6\text{H}_5\text{CH}_3$ (A) and $[\text{Co}_2(\text{hmteta})(3,6\text{-dbbq})_4] \cdot 2\text{C}_6\text{H}_5\text{CH}_3$ (B).

dence of $[\text{Co}^{\text{II}}]$ tautomer. These structural difference may be induced by the difference in electronic and steric aspects between 3,5-dbbq and 3,6-dbbq.

Magnetic Properties. The temperature-dependent (50–350 K) effective magnetic moments are shown in Fig. 3. Data were obtained for dark blue polycrystalline samples. For [3,6], $\mu_{\text{eff}}/\text{cobalt}$ was 1.8 B.M. at low temperatures (<200 K), and the effective magnetic moment drastically increased above 250 K, indicating that the compound is a $[\text{Co}^{\text{III}}]$ valence tautomer at low temperatures. That is, the $[(3,6\text{-dbsq})(3,6\text{-dbbq})\text{Co}^{\text{III}}(\text{hmteta})\text{Co}^{\text{III}}(3,6\text{-dbsq})(3,6\text{-dbbq})]$ converted into $[(3,6\text{-dbsq})_2\text{Co}^{\text{II}}(\text{hmteta})\text{Co}^{\text{II}}(3,6\text{-dbsq})_2]$ tautomer around 330 K as the temperature increased. In an earlier report, we noted

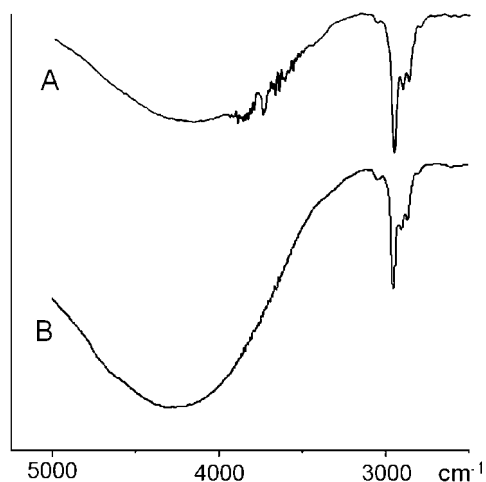


Fig. 4. IR spectra (5000–2500 cm⁻¹) of [3,5] (A) and [3,6] (B).

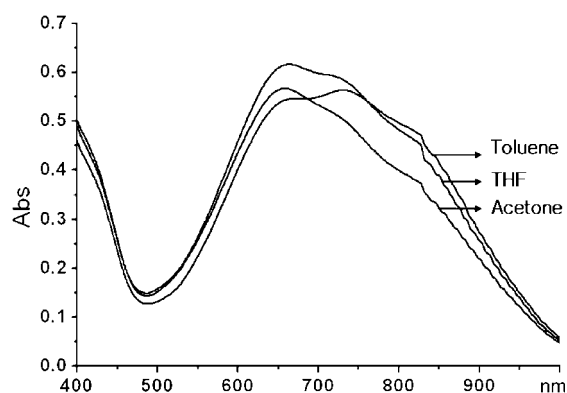


Fig. 5. Electronic absorption spectra of [Co₂(hmteta)(3,6-dbbq)₄]·2C₆H₅CH₃ in various solvents.

that the [Co^{II}(3,6-dbbq)₂(Py₂Se)] (Py₂Se = 1,1'-dipyridyl selenide) tautomer exhibits a value of 5.2 B.M.¹⁵ The effective magnetic values (μ_{eff}) of 1.7–1.8 B.M. were approximately the value expected for a $S = 1/2$ unit, which is characteristic of low spin [Co^{III}]. The $S = 3/2$ Co^{II} center couples with the two $S = 1/2$ radical semiquinonato ligands to give spin states of $S = 5/2$, $3/2$, and $1/2$. At high temperatures, μ_{eff} may be due to weak antiferromagnetic exchange between the $S = 3/2$ metal center and the two $S = 1/2$ ligands. For [3,5], the magnetic moments slowly increased in a wide range of temperatures with an increase in the temperature (2.5 B.M./cobalt at 50 K \rightarrow 3.6 B.M./cobalt at 350 K), which explains why the crystal structure at room temperature approximates to a [Co^{II}] valence tautomer. For [3,5], the reason for the slow increase in the effective magnetic moments is not clear, but the electronic effect of dissymmetric 3,5-dbbq ligand may be one of reasons. The magnetic moments of the two compounds were consistent with X-ray crystallographic data.

IR and Electronic Absorption Spectra. IR spectra in the region of 5000–2500 cm⁻¹ are shown in Fig. 4. The intensity of broad band around 4000 cm⁻¹ is dependent on the presence of [Co^{III}] tautomer.¹³ Both compounds showed a characteristic band around 4000 cm⁻¹, but their intensities were quite different: the band intensity of [3,6] was much stronger than that of [3,5], indicating that [3,6] shifted to [Co^{III}], while [3,5] shifted

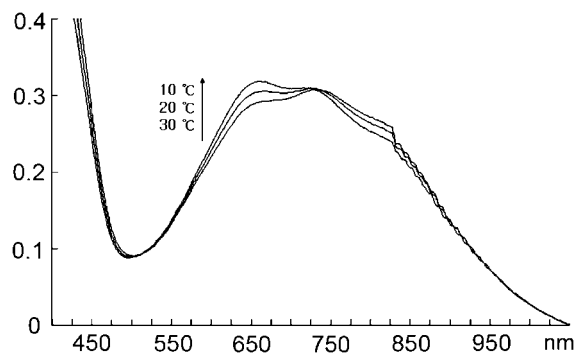


Fig. 6. Temperature-dependent electronic absorption spectra of [Co₂(hmteta)(3,6-dbbq)₄]·2C₆H₅CH₃ in toluene.

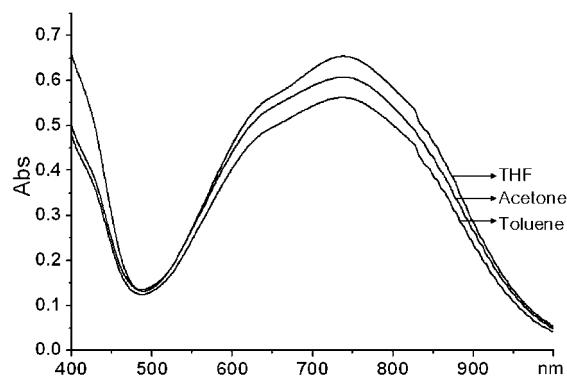


Fig. 7. Electronic absorption spectra of [Co₂(hmteta)(3,5-dbbq)₄]·C₆H₅CH₃ in various solvents.

to the [Co^{II}] tautomer in the solid state at room temperature. Such a result is consistent with the X-ray crystal structures and magnetic moments.

Electronic spectra ($\approx 10^{-4}$ M) in the range of 400–900 nm were measured. The solvent-dependent spectra of [3,6] are shown in Fig. 5. There were two bands at 640 and 740 nm, which are characteristic of [Co^{III}] and [Co^{II}], respectively.¹³ The electronic spectrum is a proof that the compound exists in an equilibrium between [Co^{III}] and [Co^{II}] in solution. The strong band at 640 nm indicated that the low spin [Co^{III}] is still a major tautomer even in tetrahydrofuran and acetone. However, the band intensity at 740 nm increased in non-polar toluene, indicating that the equilibrium shifted to [Co^{II}] species. Thus, there are significant solvent effects on the equilibrium involving [3,6]. In order to obtain the temperature effect on the equilibrium, variable temperature electronic absorption spectra (400–1000 nm) were run for [3,6] dissolved in toluene (Fig. 6). As the temperature was lowered to 10 °C, the band intensity at 640 nm increased, indicating that [Co^{III}] tautomer increases as the temperature decreased. In contrast, the spectra of [3,5], as shown in Fig. 7, indicated that [Co^{II}] was predominant even in all solutions at room temperature. The trend on the charge distribution in solution was consistent with IR, magnetic moments, and X-ray structures.

Thermal Analysis. The TGA curves of [3,5] and [3,6] are depicted in Fig. 8. For [3,5], a mass loss corresponding to the solvate toluene molecules was observed in the temperature range of 90–120 °C (obsd. 6.0%; calcd. 6.5%). The skeletal structure was stable up to 200 °C. A drastic mass loss corre-

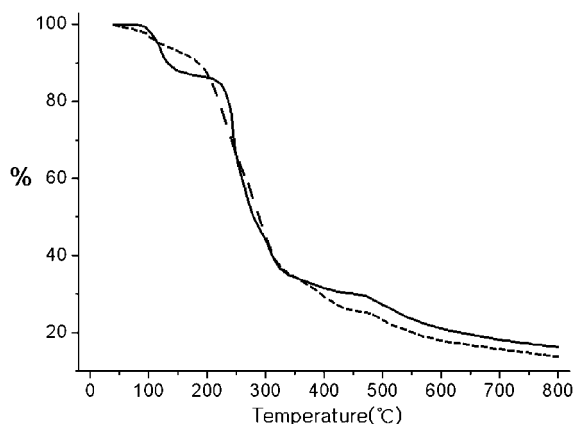


Fig. 8. TGA curves of $[\text{Co}_2(\text{hmteta})(3,5\text{-dbbq})_4] \cdot \text{C}_6\text{H}_5\text{CH}_3$ (dashed line) and $[\text{Co}_2(\text{hmteta})(3,6\text{-dbbq})_4] \cdot 2\text{C}_6\text{H}_5\text{CH}_3$ (solid line).

sponding to hmteta and 3,5-dbbq ligands was observed (obsd. 79.1%; calcd. 82.5%). For [3,6], a mass loss due to the dissociation of the solvate molecules was observed in the temperature range of 110–140 °C (obsd. 12.0%; calcd. 12.2%). The solvent-evaporation temperature was higher than that of [3,5], suggesting that the solvent molecules in [3,6] are safely nestled in the crystal lattice. Furthermore, the skeleton of the molecule was stable up to 235 °C, which is higher than that for [3,5]. The drastic loss in weight corresponding to hmteta and 3,6-dbbq ligands was observed (obsd. 76.0%; calcd. 77.6%).

Ligand and Coligand Effects for Valence Tautomerism.

Reversible valence tautomerism of the dinuclear cobalt complexes offer the potential for the design of dinuclear inorganic molecular materials with the dramatic thermochromic effects in the solid state as well as in solution. The crystal structures of both dinuclear complexes corresponded to their spectroscopic and magnetic data. The crystallographic data showed that the two cobalt ions within each dinuclear complex have the same charge distribution in the solid state at room temperature. Both complexes approximated towards $[\text{Co}^{\text{III}}]$ at low temperature and shift to $[\text{Co}^{\text{II}}]$ tautomer at high temperature. However, we do not have proof that the intramolecular two cobalt ions are different under the same conditions. There are slight differences in valence tautomerism between [3,6] and tmeda mononuclear analogue.¹³ For example, the $[\text{Co}^{\text{II}}] \rightarrow [\text{Co}^{\text{III}}]$ transition temperature (350 K) of [3,6] is much lower than that (450 K) of $[\text{Co}(\text{tmeda})(3,6\text{-dbbq})_2]$.¹³ The C–O (dbsq[−], $S = 1/2$) lengths (1.314(4) Å; 1.323(5) Å) of [3,6] are longer than the corresponding bond lengths (1.304(8) Å; 1.306(8) Å) of $[\text{Co}(\text{tmeda})(3,6\text{-dbbq})_2]$ while the C–O (dbcat^{2−}, $S = 0$) lengths (1.337(4) Å; 1.332(4) Å) are shorter than those (1.342(8) Å; 1.345(8) Å) of $[\text{Co}(\text{tmeda})(3,6\text{-dbbq})_2]$. This fact indicated that the tautomeric equilibrium of the tmeda analogue shifts towards $[\text{Co}^{\text{III}}]$ tautomer in the solid state relative to [3,6], which is well consistent with the results of the transition temperature. The difference in transition temperature between [3,6] and $[\text{Co}(\text{tmeda})(3,6\text{-dbbq})_2]$ may be ascribed to the donor nature of coligand. That is, the weak donor strength may be induced from the presence of the adjacent coordinated cobalt ion. Even though [3,5] and [3,6] did not ex-

hibit any intramolecular coupling of the two cobalt centers, in contrast to the dinuclear analogues containing a π -system,¹⁹ the subtle differences between two compounds are related to the long range electronic effects via the single bond. This emphasizes that the valence tautomerism is very sensitive to the donor nature of the coligands.

Even though [3,5] and [3,6] have the same donor coligand, the results of temperature-dependent magnetic moments, electronic absorption spectra, and IR spectra of [3,5] and [3,6] seem to reflect the subtle difference in valence tautomeric behavior. The difference between both compounds results from the isomer effect of *tert*-butyl group of dbbq ligand. According to the results, [3,6] favors $[\text{Co}^{\text{III}}]$ valence tautomer at room temperature, indicating that 3,6-dbbq^{2−} state is more stable than 3,5-dbbq^{2−} electronic state at the room temperature. The coordination character results from the ligand field environment provided by the different electronic state of two main ligands. Furthermore, the two compounds exhibited quite different solvent effects¹³ as mentioned in electronic absorption spectrum.

In conclusion, we prepared rare dinuclear valence tautomeric complexes, in which an ancillary N_4 tetradentate ligand was used as a dinuclear bridging spacer. The dinuclear cobalt complexes exhibited quite different chemistry relative to simple mononuclear analogues. For each molecule, the two intramolecular cobalt ions had the same charge distribution at room temperature. The valence tautomeric equilibrium between $[\text{Co}^{\text{III}}]$ and $[\text{Co}^{\text{II}}]$ was sensitive to the isomeric effects of main ligands as well as electronic effects of coligands. Further results will give a synthetic strategy and application of dinuclear valence tautomeric transition metal complexes.

Support for this research was provided by the University IT Research Center Project in Korea.

References

- O. Kahn, J. Kröber, C. Jay, *Adv. Mater.* **1992**, *4*, 718.
- O. Kahn, J. P. Launay, *Chemtronics* **1988**, *3*, 140.
- C. P. Berlinguette, A. Dragulescu-Andrasi, A. Sieber, J. R. Galan-Mascaros, H.-U. Güdel, C. Achim, K. Dunbar, *J. Am. Chem. Soc.* **2004**, *126*, 6222.
- A. Aviram, *J. Am. Chem. Soc.* **1988**, *110*, 5687.
- N. S. Hush, A. T. Wong, G. B. Bacskey, J. R. Reimers, *J. Am. Chem. Soc.* **1990**, *112*, 4192.
- A. Gourdon, *New J. Chem.* **1992**, *16*, 953.
- L. I. Kalontarov, *J. Phy. Chem.* **1995**, *99*, 13494.
- D. D. C. Bradley, *Chem. Br.* **1991**, 719.
- L. F. Lindoy, *Nature* **1993**, *364*, 17.
- C. G. Pierpont, C. W. Lange, *Prog. Inorg. Chem.* **1993**, *41*, 331.
- R. M. Buchanan, C. G. Pierpont, *J. Am. Chem. Soc.* **1980**, *102*, 4951.
- D. M. Adams, A. Dei, A. L. Rheingold, D. N. Hendrickson, *J. Am. Chem. Soc.* **1993**, *115*, 8221.
- O.-S. Jung, C. G. Pierpont, *Inorg. Chem.* **1994**, *33*, 2227.
- O.-S. Jung, C. G. Pierpont, *J. Am. Chem. Soc.* **1994**, *116*, 2229.
- O.-S. Jung, D. H. Jo, Y.-A. Lee, B. J. Conklin, C. G. Pierpont, *Inorg. Chem.* **1997**, *36*, 19.
- O.-S. Jung, D. H. Jo, Y.-A. Lee, H. K. Chae, Y. S. Sohn,

Bull. Chem. Soc. Jpn. **1996**, 69, 2211.

17 O.-S. Jung, Y.-A. Lee, S. H. Park, E. J. Kim, K. H. Yoo, D. C. Kim, *Bull. Chem. Soc. Jpn.* **2001**, 74, 305.

18 C. G. Pierpont, R. M. Buchanan, *Coord. Chem. Rev.* **1981**, 38, 45.

19 S. Bin-Salamon, S. H. Brewer, E. C. Depperman, S. Franzen, J. W. Kampf, K. L. Kirk, K. Kumar, S. Lappi, K. Peariso, K. E. Preuss, D. A. Shultz, *Inorg. Chem.* **2006**, 45, 4461.

20 I. S. Belostotskaya, N. L. Komissarova, E. V. Dzhuarian, V. V. Ershov, *Izv. Akad. Nauk SSSR* **1972**, 1594.

21 a) G. M. Sheldrick, *SHELXS-97: A Program for Structure*

Determination, University of Göttingen, Germany, **1997**. b) G. M. Sheldrick, *SHELXL-97: A Program for Structure Refinement*, University of Göttingen, Germany, **1997**.

22 O.-S. Jung, D. H. Jo, Y.-A. Lee, Y. S. Sohn, C. G. Pierpont, *Angew. Chem., Int. Ed. Engl.* **1996**, 35, 1694.

23 O.-S. Jung, Y. T. Kim, Y.-A. Lee, Y. J. Kim, H. K. Chae, *Inorg. Chem.* **1999**, 38, 5457.

24 D. L. Keppert, *Prog. Inorg. Chem.* **1977**, 1, 23.

25 J. A. Bertrand, J. A. Kelly, E. G. Vassian, *J. Am. Chem. Soc.* **1969**, 91, 2394.